

**Computational and Biological Evaluation of the Soybean Lecithin-Gallic Acid
Complex for Ameliorating Alcoholic Liver Disease in Mice with Iron Overload**

Xiangqun Wu¹, Yan Wang², Ran Jia³, Fang Fang^{1*}, Ya Liu^{1*} and Weiwei Cui^{1*}

¹ Department of Nutrition and Food Hygiene, School of Public Health, Jilin University,
Changchun, P. R. China.

² Institute of Biomedical and Pharmaceutical Sciences, Guangdong University of
Technology, Higher Education Mega Center, Guangzhou, P. R. China.

³ State Key Laboratory of Theoretical and Computational Chemistry, Institute of
Theoretical Chemistry, Jilin University, Changchun, P. R. China.

***Corresponding Authors:**

* **Weiwei Cui:** Department of Nutrition and Food Hygiene, School of Public Health,
Jilin University, Changchun, P. R. China.

* **Fang Fang:** Department of Nutrition and Food Hygiene, School of Public Health,
Jilin University, Changchun, P. R. China.

* **Ya Liu:** Department of Nutrition and Food Hygiene, School of Public Health, Jilin
University, Changchun, P. R. China.

Authors' Email Addresses:

Weiwei Cui: Tel: +86-431-8561-9455

E-mail: cuiweiwei@jlu.edu.cn

Fang Fang: Tel: +86-431-8561-9455

E-mail, fangfang7786@jlu.edu.cn

Ya Liu: Tel: +86-431-8561-9455

E-mail, liuya@jlu.edu.cn

1 **Materials and Methods**

2 **Measurement of gallic acid content and complexing rate**

3 A high-performance liquid chromatograph (Waters 600 HPLC, Waters
4 Corporation, Milford, MA, US) was used to measure the gallic acid (GA) content in the
5 eluate and to calculate the complexing rate. The chromatographic conditions were as
6 follows: analytical HPLC was carried out with diode array detection at 283 nm on an
7 Agilent HC-C18 column (250 mm × 4.6 mm, 5 μm) with isocratic elution in 80%
8 acetonitrile/20% water (0.1% formic acid), column temperature at 25°C, and feeding
9 of 20 μL.

10

11 **Ultraviolet spectrum analysis**

12 Solutions of samples to be measured were scanned at wavelengths of 200–400 nm
13 for the ultraviolet spectrum analysis (UV-3600 ultraviolet-visible Spectrophotometer,
14 Shimadzu, Japan).

15

16 **Differential thermal analysis**

17 The temperature was increased by 5°C every minute over a measurement range of
18 50°C–800°C, and GA, soybean lecithin, the soybean lecithin-GA complex (SL-GAC),
19 and a physical mixture of soybean lecithin and GA were analyzed using differential
20 scanning calorimetry (DSC; Heson, Shanghai, China).

21

22 Computational methods

23 **1. Construction of lecithin and GA molecules.** The atomic coordinates of the lecithin
24 molecule were extracted from the crystal structure of human phosphatidylcholine
25 transfer protein (hPTP; PDB ID: 1LN1). GA was built with the aid of Discovery Studio
26 v4.0 Visualizer. Both molecules were optimized using the
27 Gaussian v09 software package under the 6-311+g(d,p) basis set by the B3LYP
28 method.¹ The optimized structures of the lecithin and GA molecules were used for the
29 subsequent studies.

30

31 **2. Generation of the structure of SL-GAC.** Gaussian-accelerated molecular dynamics
32 (GaMD) is a biomolecular enhanced-sampling method that works by adding a harmonic
33 boost potential to smoothen the system potential energy surface.² Without the need to
34 set predefined reaction coordinates, GaMD enables unconstrained enhanced sampling
35 of biomolecules. This method can also be applied to sample the binding mode between
36 two molecules, such as the lecithin and GA molecules. The structure of SL-GAC is
37 unknown. It has been reported that in this complex, GA and lecithin combine via a non-
38 covalent bond and do not form a new compound.³ Therefore, we can employ GaMD to
39 sample the non-covalent complex of lecithin and GA. The optimized structures of the
40 lecithin and GA molecules were first placed randomly, and the centroid distance
41 between these two molecules was approximately 50 Å. Then, these two molecules were
42 solvated in an octahedral periodic box by using the TIP3P water model. The distance

43 between the outermost lecithin and GA atoms, and the walls of the simulation box was
44 set to 10.0 Å. Then, GaMD simulation was performed for a total of 2 μs for the lecithin
45 and GA systems, and this generated 100,000 frames. The GaMD simulation was
46 conducted using the AMBER v16 software package.⁴

47

48 **3. Construction of lecithin-GA-human phosphatidylcholine transfer protein**

49 **complex.** By performing GaMD on the lecithin and GA molecules, we obtained the
50 non-covalent complex of lecithin and GA. To determine how this non-covalent
51 complex interacted with the target protein, we used the molecular docking method to
52 construct a complex structure of lecithin-GA-hPTP. The atomic coordinates of hPTP
53 were extracted from its crystal structure (PDB ID: 1LN1). The lecithin molecule in this
54 crystal structure was removed, and the non-covalent complex of lecithin and GA
55 obtained from the GaMD simulation was docked into the active site of 1LN1. The
56 molecular docking was conducted using the AutoDock v4.2 software package.⁵ The
57 nonpolar hydrogen atoms were removed, and only the polar hydrogens were retained.
58 Gasteiger charges were added to the hPTP and non-covalent lecithin-GA complex. A
59 box size of $40 \times 40 \times 40$ Å³ with a grid spacing of 0.375 Å was defined around the
60 binding site of hPTP, so that it contained all the residues that are critical for interacting
61 with the non-covalent complex. The grid map around the binding site of hPTP was
62 generated using the probe atoms and the Auto Grid program. Each grid in the map
63 represented the potential energy of a probe atom in the presence of all the atoms of the

64 receptor molecule. The Lamarckian genetic algorithm was used for the docking study.
65 One hundred runs with 15,000,000 maximum evaluations and 270,000 generations
66 were used for the docking simulation. The docking pose with the lowest binding energy
67 ($-5.67 \text{ kcal mol}^{-1}$) was chosen as the starting structure for the subsequent molecular
68 dynamic (MD) simulation.

69

70 **4. MD simulation of hPTP and lecithin-GA complex structure**

71 Based on the complex structure obtained using the molecular docking, MD
72 simulation was carried out. To determine how the lecithin-GA complex affected the
73 structure of hPTP, we constructed two systems: an hPTP-only system that contained no
74 ligand (denoted as apo-hPTP) and hPTP complexed with lecithin and GA (denoted as
75 complex-hPTP). All MD simulations were carried out using the AMBER v16 software
76 package.⁴ All the missing hydrogen atoms of the hPTP protein were added using the
77 LEaP module. The ff14SB force field was applied for the hPTP protein.⁶ The parameter
78 sets for the lecithin and GA molecules were supplied by the general AMBER force
79 field.⁷ Sodium ions were added to the complex systems by using a coulomb potential
80 grid to keep the whole system neutral. According to the experimental process, the mice
81 were fed an excess amount of alcohol. To simulate this condition, the apo-hPTP and
82 complex-hPTP structures were solvated by water and ethanol molecules. The TIP3P
83 water model and ethanol molecules were employed to solvate the two systems.⁸ Both
84 systems were solvated in an octahedral periodic box. The distance between the

85 outermost protein atoms and the walls of the simulation box was set to 10.0 Å. Each
 86 system was first submitted to 4000 steps of steepest-descent minimization and then to
 87 6000 steps of conjugate-gradient minimization. Subsequently, the two systems were
 88 heated from 0 to 310 K in 500 ps. The heating process was conducted under the
 89 canonical ensemble (NVT ensemble). A harmonic restraint with a force constant of
 90 10.0 kcal mol⁻¹ Å⁻² was applied to the whole system. A Langevin thermostat was used
 91 during the heating process. Then, under an NPT ensemble with constant pressure (1.0
 92 bar), the two systems were equilibrated for 5 ns. The relaxation time for the barostat
 93 bath was set to 2.0 fs. In the end, the apo-hPTP and complex-hPTP systems were both
 94 simulated for 200 ns. The NPT ensemble was used for this process, and periodic
 95 boundary conditions were employed. The long-range electrostatics was handled using
 96 the particle-mesh Ewald method.⁹ The cut-off value for short-range interactions was set
 97 to 10.0 Å. The SHAKE algorithm was employed to constrain bonds involving
 98 hydrogen. The time step for all the simulations was set to 2 fs.

99

100 **5. Calculation of binding free energies**

101 The molecular mechanics/generalized Born surface area (MM/GBSA) method was
 102 implemented using AMBER v16 to calculate the binding free energy between SL-GAC
 103 and hPTP.^{10, 11} The binding free energy (ΔG_{bind}) in MM/GBSA between a ligand (L) and
 104 a receptor (R) to form a complex RL was calculated as follows:

$$105 \quad \Delta G_{bind} = G_{complex} - (G_{receptor} + G_{ligand}) \quad (1)$$

$$G = E_{MM} + G_{sol} - TS \quad (2)$$

$$E_{MM} = E_{int} + E_{ele} + E_{vdw} \quad (3)$$

$$G_{sol} = G_{GB} + G_{SA} \quad (4)$$

In eqn (2), E_{MM} , G_{sol} , and TS represent the molecular mechanics component in the gas phase, the stabilization energy due to solvation, and a vibrational entropy term, respectively. E_{MM} is given as the sum of E_{int} , E_{ele} , and E_{vdw} , which are internal, Coulomb, and van der Waals interaction terms, respectively. The solvation energy, G_{sol} , is separated into an electrostatic solvation free energy (G_{GB}) and a nonpolar solvation free energy (G_{SA}). The former can be obtained using the Generalized Born (GB) method. The latter is considered to be proportional to the molecular solvent accessible surface area.¹² The binding free energies were obtained by averaging the values calculated for 5000 frames from the last 50 ns of the trajectories at 5-ps intervals for the complex structure.

119

120 **Acute toxicity study**

The principles of laboratory animal care were followed, and all procedures were conducted according to the guidelines established by the National Institutes of Health. Every effort was made to minimize suffering. This study was approved by the Animal Experiment Committee of Jilin University. A total of 20 healthy ICR mice (10 male, 10 female) weighing 20.0 ± 2.0 g were supplied by the Experimental Animal Center of Public Health College, Jilin University (Jilin, China). All mice were accommodated

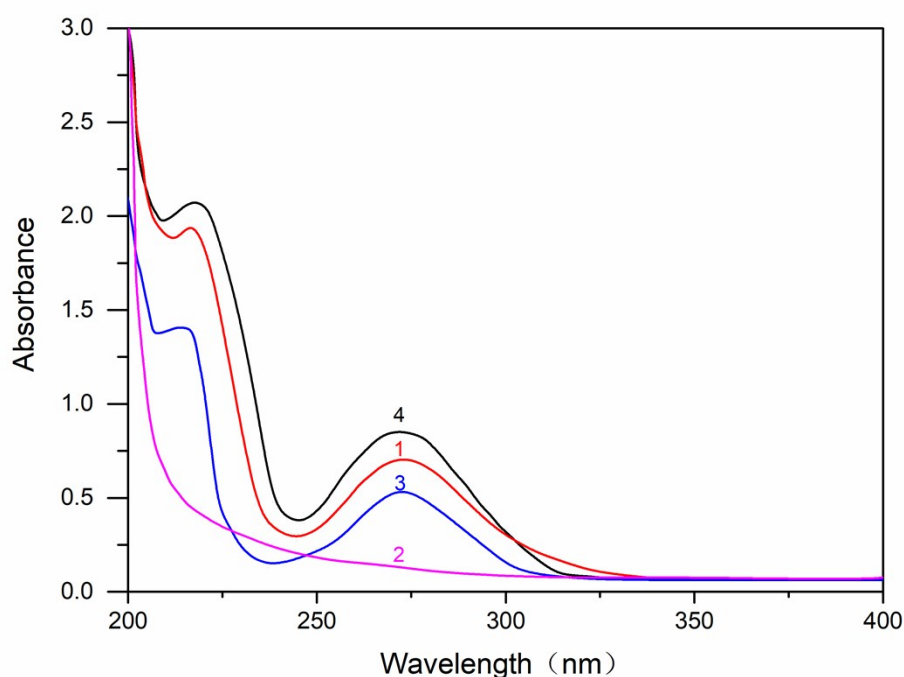
under the following conditions: room temperature, $25^{\circ}\text{C} \pm 2^{\circ}\text{C}$; relative humidity, 60% $\pm 10\%$; room air changes, 12–18 times/h; and a 12-h light/dark cycle. Throughout the study, the mice were fed a normal chow diet and purified water ad libitum. However, they were fasted for 6 h prior to the oral administration. The test was conducted according to OECD guidelines.¹³ The animals were randomly divided into 2 groups of 10 mice each, including 5 animals of each sex. SL-GAC was suspended in purified water, and was administered at a dose of 5000 mg/kg bodyweight (BW) by gavage to the mice in the experimental group. The other group served as the control. After the administration of SL-GAC, the clinical symptoms of the mice were observed immediately after dosing, at 6 h, and at 24-h intervals, and then at 24-h intervals for 7 days. Clinical symptoms, including mortality, clinical signs, and gross findings, were recorded. On day 7, the mice were sacrificed by cervical dislocation and examined by necropsy.

Results

Ultraviolet spectrum analysis

From the ultraviolet (UV) diagrams for GA, soybean lecithin, SL-GAC, and soybean lecithin-GA physical mixture (Fig. S1), we found that lecithin did not have a characteristic absorption peak within the scope of the scanning wavelength. GA had its maximum absorption peak at a wavelength of 272 nm. The physical mixture and the complex also had maximum absorption peaks with the same wavelengths, but the peak of the complex was not as high as that of GA at the same concentration. This proved that the complex had not resulted in any changes to the chemical structure of GA.

149 Furthermore, the complex mainly showed the chemical properties of GA. The decrease
150 in its characteristic peak may be because the characteristic structure was involved in
151 the SL-GAC.



152 **Figure S1.** Ultraviolet spectrum curves of GA (1), soybean lecithin (2), SL-GAC (3),
153 and the physical mixture of gallic acid and soybean lecithin (4)

154

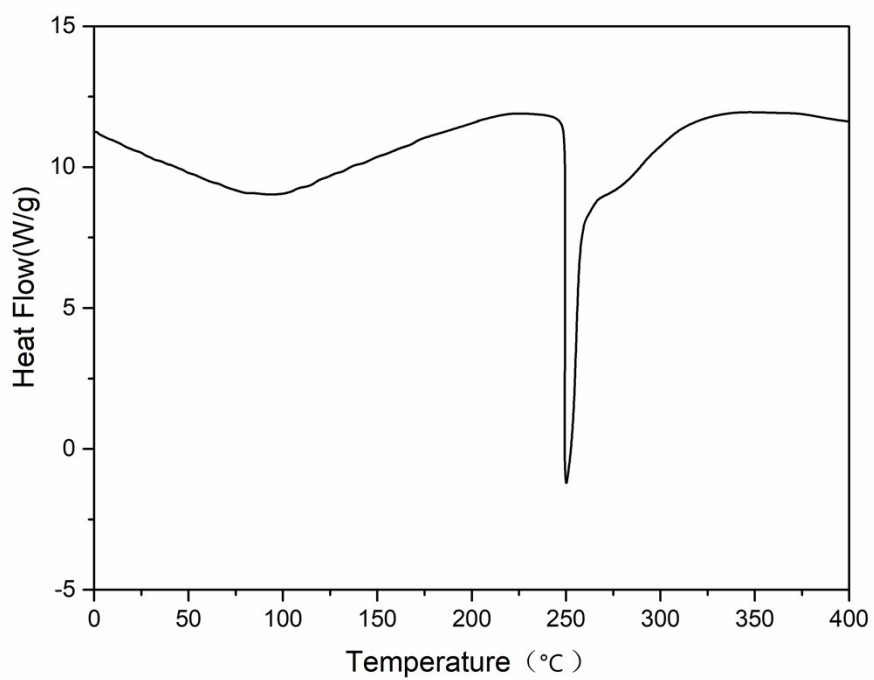
155 **Differential thermal analysis**

156 As indicated by the differential scanning calorimeter (DSC) diagram of GA,
157 soybean lecithin, and their mixture and complex (Fig. S2–S5), GA began to have an
158 absorption peak at 250°C, which corresponds to its melting point (Fig. S2). With an
159 amorphous form, soybean lecithin had no definite melting point and had a large
160 absorption peak at 276°C and two small absorption peaks at 207.2°C and 381.5°C each

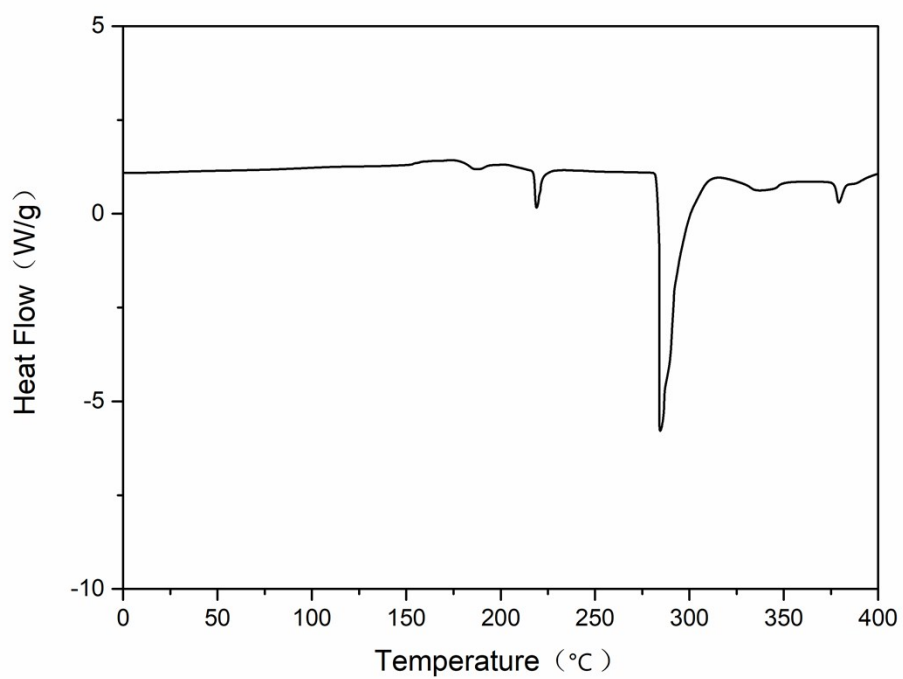
161 (Fig. S3). The small peak at 207.2°C may have been caused by the polar end of lecithin,
162 whereas the latter two peaks were caused by a change in the physical phase from gel to
163 liquid as the long chain between carbon and hydrogen was broken or separated. The
164 melting peak of GA in the complex disappeared completely, and in general, its DSC
165 diagram was very similar to that of lecithin; however, the heat absorption peak appeared
166 at a lower temperature, which indicated that GA no longer existed in the form of
167 crystals, and was instead completely dispersed in lecithin (Fig. S4). The reason for this
168 is probably because the polar ends of the GA and lecithin molecules were combined,
169 which degraded the orderliness among the aliphatic hydrocarbon chains of lecithin. The
170 DSC diagram of the GA-soybean lecithin physical mixture mainly showed a
171 superposition of the diagrams of the two molecules, and the melting peak of GA could
172 still be observed (Fig. S5).

173

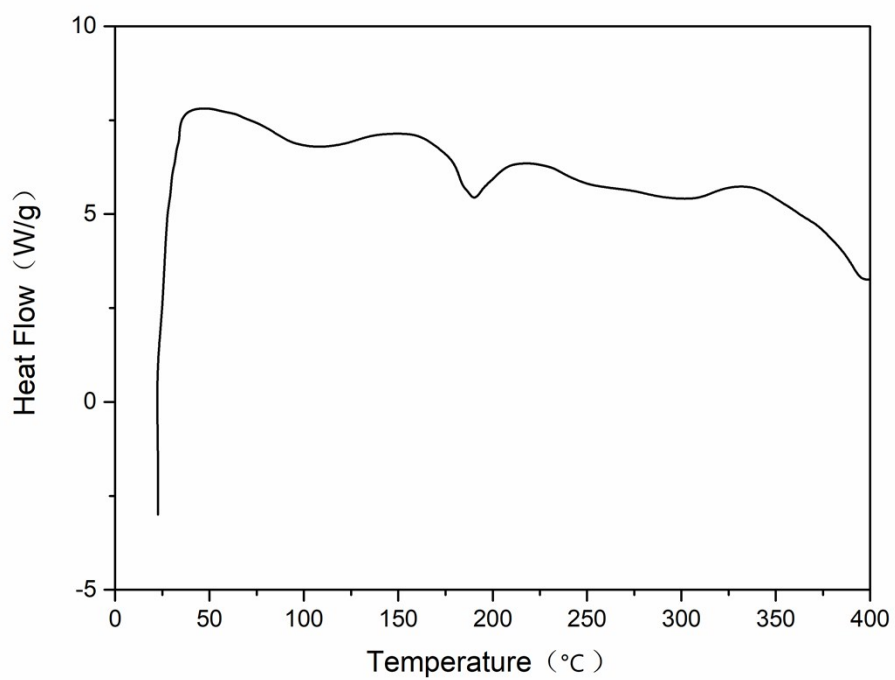
174



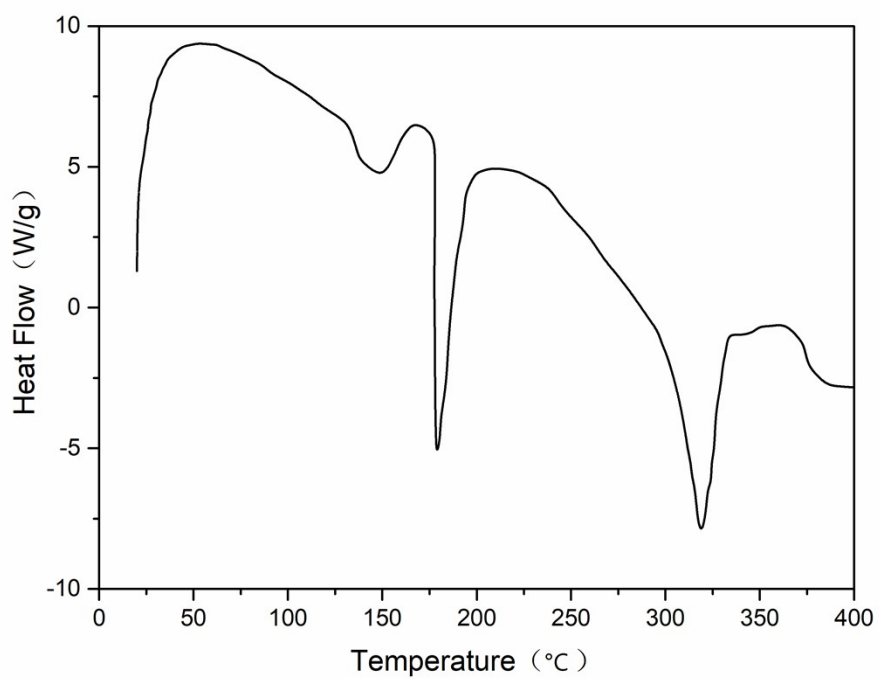
175 **Figure S2.** Differential scanning calorimetry curve of GA



176 **Figure S3.** Differential scanning calorimetry curve of soybean lecithin

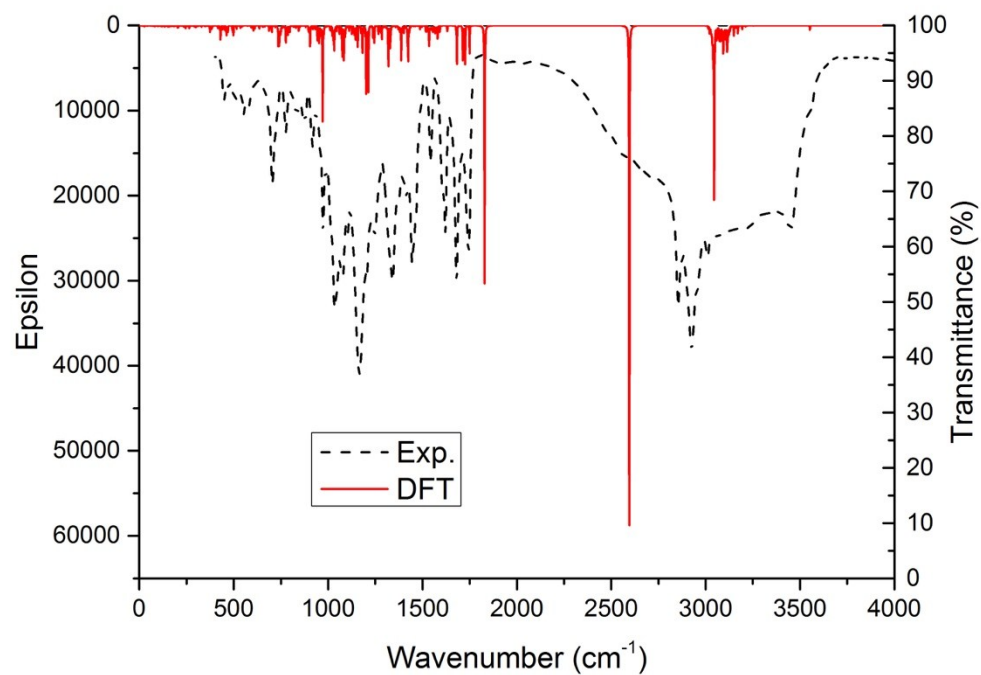


177 **Figure S4.** Differential scanning calorimetry curve of SL-GAC

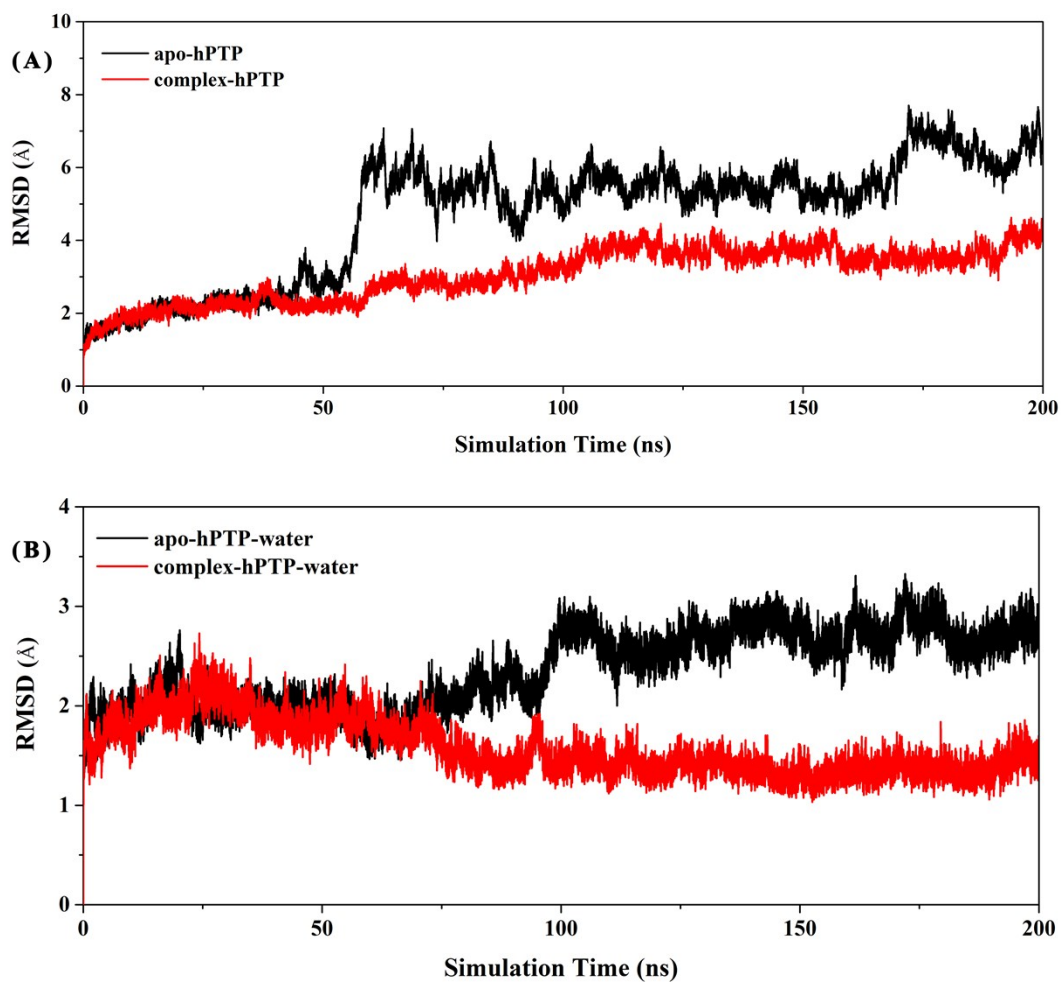


178 **Figure S5.** Differential scanning calorimetry curve of the physical mixture of GA and
 179 soybean lecithin
 180

181 **Computer simulations**



182 **Figure S6.** Computational infrared (IR; red lines) and experimental IR (black dashed
183 lines)



184 **Figure S7.** Root means square deviation (RMSD) plots for apo-hPTP and complex-
 185 hPTP in both (A) ethanol and (B) water
 186

Table S1. Hydrogen-bond analysis between the hydroxyl group of GA and the phosphate group of lecithin

Donor	Acceptor	Average distance (Å)	Average angle (°)	Percentage (%)
O5@lecithin	H2@gallic acid	1.64	166.77	100
O5@lecithin	H3@gallic acid	1.68	165.42	100

Table S2. Binding free energies (kcal·mol⁻¹)

	ΔG_{VDW}	ΔG_{ele}	ΔG_{GB}	ΔG_{SURF}	ΔG_{TOT}	$T\Delta S$	$\Delta G_{binding}$
Ethanol	-102.60	-31.80	69.00	-14.70	-80.098	-48.55	-31.55 ± 8.98
Water	-108.37	-51.55	88.61	-15.25	-86.56	-38.88	-47.68 ± 7.85

Acute toxicity of SL-GAC

The clinical symptoms of mice were observed for 7 days after the intragastric administration of SL-GAC. All of the mice administered SL-GAC at a dose of 5000 mg/kg survived the 7-day observation period. There were no clinical signs of toxicity throughout the experimental period. The administration of SL-GAC did not cause any appreciable alteration in the mean body weights of the mice.

To determine the safety of SL-GAC, we performed an oral acute toxicity test. The absence of any adverse effects after the administration of a dose of 5000 mg/kg clearly indicated the non-toxic nature of SL-GAC. Toxicologists agree that any test substance that is not lethal when administered as a single oral dose at a concentration of 5000 mg/kg is essentially non-toxic.^{13, 14} Therefore, it may be concluded that SL-GAC was practically non-toxic and was safe via the oral route.

208 **Table S3.** Body weight of SL-GAC-fed mice in the acute toxicity study (g/mouse)

	Time (day)						
	1	2	3	4	5	6	7
Control	18.7 ± 0.8	20.4 ± 1.1	20.7 ± 1.5	21.1 ± 1.8	21.7 ± 2.2	22.3 ± 2.6	22.9 ± 2.8
SL-GAC	17.2 ± 1.1	18.4 ± 1.2	19.2 ± 1.3	20.0 ± 1.5	20.8 ± 1.6	21.7 ± 1.7	22.6 ± 2.1

209

210

REFERENCES

- 211 1. M. J. Frisch, G. Trucks, H. Schlegel, G. Scuseria, M. Robb, J. Cheeseman, G.
212 Scalmani, V. Barone, B. Mennucci and G. Petersson, Gaussian 09, Revision D.
213 01, Gaussian, Inc.: Wallingford, CT, 2009.
- 214 2. Y. Miao, V. A. Feher and J. A. McCammon, Gaussian Accelerated Molecular
215 Dynamics: Unconstrained Enhanced Sampling and Free Energy Calculation, *J*
216 *Chem Theory Comput*, 2015, **11**, 3584-3595.
- 217 3. C. Liu, C. Chen, H. Ma, E. Yuan and Q. Li, Characterization and DPPH Radical
218 Scavenging Activity of Gallic Acid-Lecithin Complex, *Tropical Journal of*
219 *Pharmaceutical Research*, 2014, **13**, 1333-1338.
- 220 4. D. S. C. D.A. Case, T.E. Cheatham, III, T.A. Darden, R.E. Duke, T.J. Giese, H.
221 Gohlke, A.W. Goetz, D. Greene, N. Homeyer, S. Izadi, A. Kovalenko, T.S. Lee,
222 S. LeGrand, P. Li, C. Lin, J. Liu, T. Luchko, R. Luo, D. Mermelstein, K.M.
223 Merz, G. Monard, H. Nguyen, I. Omelyan, A. Onufriev, F. Pan, R. Qi, D.R.
224 Roe, A. Roitberg, C. Sagui, C.L. Simmerling, W.M. Botello-Smith, J. Swails,
225 R.C. Walker, J. Wang, R.M. Wolf, X. Wu, L. Xiao, D.M. York and P.A.
226 Kollman AMBER 16, University of California, San Francisco, 2016.
- 227 5. G. M. Morris, R. Huey, W. Lindstrom, M. F. Sanner, R. K. Belew, D. S.
228 Goodsell and A. J. Olson, AutoDock4 and AutoDockTools4: Automated
229 docking with selective receptor flexibility, *J Comput Chem*, 2009, **30**, 2785-
230 2791.
- 231 6. J. A. Maier, C. Martinez, K. Kasavajhala, L. Wickstrom, K. E. Hauser and C.
232 Simmerling, ff14SB: Improving the Accuracy of Protein Side Chain and
233 Backbone Parameters from ff99SB, *J Chem Theory Comput*, 2015, **11**, 3696-
234 3713.
- 235 7. J. Wang, R. M. Wolf, J. W. Caldwell, P. A. Kollman and D. A. Case,
236 Development and testing of a general amber force field, *J Comput Chem*, 2004,
237 **25**, 1157-1174.
- 238 8. W. L. Jorgensen, J. Chandrasekhar, J. D. Madura, R. W. Impey and M. L. Klein,
239 Comparison of simple potential functions for simulating liquid water, *The*
240 *Journal of Chemical Physics*, 1983, **79**, 926-935.
- 241 9. T. Darden, D. York and L. Pedersen, Particle mesh Ewald: An N·log(N) method
242 for Ewald sums in large systems, *The Journal of Chemical Physics*, 1993, **98**,
243 10089-10092.

- 244 10. Y. Wang, W. S. Cai, L. Chen and G. Wang, Molecular dynamics simulation
245 reveals how phosphorylation of tyrosine 26 of phosphoglycerate mutase 1
246 upregulates glycolysis and promotes tumor growth, *Oncotarget*, 2017, **8**,
247 12093-12107.
- 248 11. J. M. J. Swanson, R. H. Henchman and J. A. McCammon, Revisiting Free
249 Energy Calculations: A Theoretical Connection to MM/PBSA and Direct
250 Calculation of the Association Free Energy, *Biophys J*, 2004, **86**, 67-74.
- 251 12. T. Hou, W. Zhang, D. A. Case and W. Wang, Characterization of Domain-
252 Peptide Interaction Interface: A Case Study on the Amphiphysin-1 SH3
253 Domain, *J Mol Biol*, 2008, **376**, 1201-1214.
- 254 13. OECD, *Guidance Document on the Recognition, Assessment and Use of*
255 *Clinical Signs as Human Endpoints for Experimental Animals Used in Safety*
256 *Evaluation*, 2002.
- 257 14. Anon, Code of Federal Regulations, Title 40, Part 158, 1985.

258